CrossMark

ORIGINAL PAPER

Application of probabilistic neural network with transmission and distribution protection schemes for classification of fault types on radial, loop, and underground structures

Atthapol Ngaopitakkul[1] · Monthon Leelajindakrairerk[1]

Abstract This paper proposes the development of transmission and distribution protection schemes to classify faults along transmission and distribution systems. The systems under consideration are composed of a 500-kV radial (two-bus single circuit), loop (three-bus double circuit) structure transmission systems, and a 115-kV radial structure underground distribution system. This complex system shows the advantage of the proposed method. A decision algorithm based on a discrete wavelet transform (DWT) and probabilistic neural network is investigated for inclusion in a transmission and distribution protection system. Fault signals in each case are extracted to several scales on the DWT to decompose high-frequency components from fault signals using the mother wavelet daubechies4. The maximum coefficients of a DWT at 1/4 cycle that can detect faults are used as input patterns for the training process in a decision algorithm. In addition, coefficients from a DWT technique and a back-propagation neural network algorithm are also compared with the proposed algorithm in this paper. Moreover, the real signal from an experimental set-up was investigated. Based on the accurate results for the simulation signal and real signal, it can be concluded that the proposed algorithm is adequate for other power systems with different line models and that it can be applied to actual systems even if the accuracy is slightly reduced by the effect of noise in an actual system. Thus, the overall results show that the proposed algorithm can detect a faulty bus and classify types of fault with satisfactory results.

✉ Atthapol Ngaopitakkul
   atthapol.ng@kmitl.ac.th

[1] Department of Electrical Engineering, Faculty of
    Engineering, King Mongkut's Institute of Technology
    Ladkrabang, Bangkok 10520, Thailand

1 Introduction

Power systems normally contain a large number of transmission lines, busbars, generations, transformers, and protective devices. The occurrence of a fault on a major transmission line may endanger the operation of many power systems and potentially lead to charge outages. If fault diagnosis results are not available to system operators shortly after a fault occurs, it may not be possible to reach an optimal decision to restore the power system. Fault diagnosis normally depends on the knowledge of the power system. The power system status must be clarified before restorative actions can occur. Fault diagnosis systems identify the location and type quickly and accurately. Generally, fault detection and classification can be described by this knowledge.

A fault inception instant is detected by looking for an abrupt change in signal waveforms. A decrease in a voltage waveform indicates the possible faulted phases. The current experiencing the highest increase in amplitude indicates a probable faulted circuit. The overall change in voltage and current waveforms indicates the type of fault, such as a single line-to-ground fault or a three-phase fault. Fault diagnosis involves the identification of the fault location and fault type (sometimes called "fault classification"). When the fault event is complex, it may not be possible for a fault diagnosis system to identify the exact fault location and fault type. This can occur when the protective devices malfunction, including the wrong tripping zone, failure to trip, misoperation, improper operating time, and wrong direction of the fault. Conventional methods such as overcurrent, distance, and directional relays are still utilized for the fault diagnosis

🖄 Springer

of transmission systems used by the Electricity Generating Authority of Thailand (EGAT).

Fault classification for conventional protection was proposed with Fourier transforms based on variations in the voltage and current of the three phases. Fault classification is designed to analyse or identify the types of fault that occur, such as single line-to-ground, double line-to-ground, line-to-line, and three-phase faults. The variation in the voltage and current of the three phases using Fourier transforms is very effective in identifying the type of fault. However, the traditional method of signal analysis, which is based on Fourier transforms, is not very efficient for this type of study because the generated fault signals are nonstationary transient. Thus, the Fourier transform algorithm uses data of the current with a time of one cycle for the analysis. Moreover, there are certain factors that can cause needless operation of distance protection, including current transformer (CT) saturation, the resistances of fault arcs, impedance data, and calculation errors. To avoid the malfunction of the distance relay in these cases, several algorithms [1–41] have been developed for the protective relays.

In the literature for fault detection algorithms [1–16], there are several decision algorithms that were developed for use in protective relays to prevent unnecessary operation of the protective equipment under different nonfault conditions. The fast Fourier transform (FFT) [1], discrete wavelet transform (DWT) [2–6], artificial neural networks (ANNs) [7], transient-based protection [8,9], and hybrid systems [10] have been used in fault diagnosis. In [1], the researchers presented fault detection in rotating machines using an FFT-based discrete harmonic wavelet. In [2], the researchers discussed voltage disturbance detection in distribution systems using a wavelet transform with a negative selection artificial immune algorithm. A finite impulse response (FIR) filter is applied to extract pure fault characteristics. The simulation showed that the proposed approach is effective in detecting and identifying various types of faults. In [11], the researchers presented fault detection for a grid consisting of an offshore wind farm. A retrieve signal was applied by empirical mode decomposition (EMD) to extract the magnitude and phase angle. This approach was applied for fault detection in an AC/DC network section with a demonstration using a real-time digital simulator to verify the performance of the algorithm.

Research by Yao et al. [3] presented a detection algorithm for DC arc faults using a wavelet transform. An experimental set-up was built to evaluate DC arc characteristics and factors that affect the DC voltage source, arc length, and arc level. The proposed algorithm used a current change in the time domain and normalized RMS value from a wavelet transform. In [4], the researchers proposed fault detection using a wavelet-based algorithm and applied the proposed system to a 282-bus radial distribution system.

Alshareef et al. [7] applied a wavelet to islanding detection of distributed generation. This new approach uses a newly designed wavelet and support vector machine classifier to filter coefficients. Real-time detection of an induced transient is presented in [8]. The proposed methodology consists of a new decomposition process using the time domain instead of one wavelet coefficient. Simulations of a fault, high-impedance fault, and PQ disturbance are conducted to evaluate the performance of the proposed algorithm and to reveal a satisfactory result. For a microgrid system, research by Li et al. [12] discussed a protection algorithm using mathematical morphology (MM) technology. It can operate with fast response and can be applied to various topologies and operation modes. A fault location method for a low-voltage distribution system using time-based methodology was proposed in [13]. An impedance-based algorithm combined with a time-based three-phase load flow was used to increase accuracy and reduce time for detection. The algorithm uses the border effects of sliding windows; thus, the choice of mother wavelet and fault parameters does not affect performance.

The application of a DWT and support vector machine for fault diagnosis and monitoring using an induction machine was presented in [10]. In [5], the research proposed a DWT-based method to detect outer cage faults in double squirrel-cage induction motors (DCIMs) that can operate under transient conditions. The proposed technique is an effective tool for estimating fault severity, and it can provide solutions to difficulties in detecting faults in the outer case of a DCIM using steady-state spectrum analysis. In [14], the researchers discuss various techniques using wavelet based for fault detection in a high-voltage transmission line. The application of a stationary wavelet transform (SWT) and DWT in fault detection and fault phase identification in a three-phase induction motor is presented in [6]. In [15], the researchers introduce an ultra-high-speed protection scheme based on comparing the amplitudes of the initial travelling waves detected in the currents of the parallel circuits. This discriminates the internal faults and classifies the faulted phases. A time-shift invariant property of a sinusoidal waveform is used in [16] for an ultrafast classification of fault types in a power transmission line. The performance of the proposed scheme is compared in terms of group delays and data windows with other feature extractions such as fuzzy logic, HS transform, DWT, and discrete Fourier transform.

Because of transient-based techniques [17–33], the advantage of a wavelet transform is that the band of analysis can be adjusted to allow high-frequency and low-frequency components to be precisely detected. The idea of applying a wavelet transform to fault diagnosis is not new, and there are a number of research papers exploring the concept [18–28]. Fault location methodology using a single-ended travelling wave was presented in [27]. The methodology using DWT and support vector machine to identify fault sections has the advantages

of small inputs and being independent of fault types. The application of a hybrid transmission line consists of overhead and underground cables. The application of a wavelet transform in fault classification was initially proposed in the literature by Youssef [18]. For a generator, wavelet analysis can be applied in order to detect, identify, and classify faults as discussed in [29]. Two common types of fault in an induction generator were investigated, including the interturn short-circuit fault (ITSCF) and winding resistive asymmetrical fault (WRAF).

A new fault diagnostic index (FDI) using wavelet-based analysis exhibited efficiency and accuracy in fault discrimination. In [30], the researchers discussed the application of wavelet-based signal processing in a high-impedance grounded distribution network, and the difficulty in identifying a single line-to-ground fault with weak characteristics and noise signals. Guillen et al. [31] discussed an algorithm based on a DWT and singular value decomposition. The proposed methodology showed promise in reducing the computational burden and detection time. An application of multisolution wavelet analysis to transmission line fault classification is discussed in [32]. A regression tree algorithm was used to classify islanding conditions. The proposed algorithm was compared with various techniques in the past to verify performance.

The application of a wavelet-based algorithm for fault detection and identification in transmission lines with demonstrated hardware was presented by Usama et al. [25]. Another research study by Dasgupta et al. [26] presented fault location and classification using a wavelet transform and an ANN. A comparison between various wavelet-based algorithms was conducted in terms of time and accuracy, and the proposed method was successful in classifying and locating faults. In [27], researchers proposed using a DWT and support vector machine to locate faults in a transmission line consisting of overhead lines and underground cables. The performance of the algorithm was tested on various fault scenarios with satisfactory results.

Based on a comparison of the coefficients detail of DWT, considering the pattern of the spectra, which was developed by Markming et al. [19], a comparison of the coefficients from the first scale that can detect a fault is considered. A division algorithm between the maximum coefficients of DWT at a 1/4 cycle of phases A, B, and C is performed in a single-circuit radial structure transmission system. To identify the phase with faults, comparisons of the maximum ratio obtained from a division algorithm were conducted so that the types of faults could be analysed. In several research papers, fault current signals are decomposed into various scales of wavelet transforms. By considering the pattern of the spectra, fault classification can be conducted by employing a trial-and-error method [18,19,32]. A transmission line protection scheme combining two protection functions (a directional-zone function and fault classification function based on an adaptive wavelet and Bayesian rules) was investigated by Perez et al. [22]. The results demonstrated that a directional-zone function can determine whether the fault is backward, inside, or forward the primary protected line. On the other hand, the fault classification function can distinguish faults of different types regardless of fault resistance values.

In addition, in the literature for fault classification [19,34–40], most researchers have only considered fault classification for single-bus and two-bus systems. ANN techniques have been proposed in some approaches in the literature to improve transmission and distribution protection [34–37] because these algorithms can give precise results. In [38], researchers proposed an alternative approach for fault location using a fault locator based on feedforward ANNs. The algorithm was applied to an overhead power distribution feeder using a CAD simulation. The results showed satisfactory performance compared with the conventional method. In [39], researchers applied a Chebyshev neural network for fault classification in a series compensate transmission line. The proposed algorithm has a single-layer structure; thus, it is easy to implement and has proven to be immune to measurement errors and noise. A multiwavelet packet and radial basis function (RBF) neural network also showed promising results, with the ability to recognize and classify various types of fault in transmission lines satisfactorily and efficiently [40].

Research by Liu et al. [40] proposed multiwavelets and radial basis function neural networks to classify faults in a transmission line. The advantage is that a multiwavelet can process orthogonality, and there is more low- and high-frequency information for classification, as experimental results from the paper showed. Another application is an induction machine using a complex wavelet-based probabilistic neural network to diagnose interturn faults [41]. The BPNN is a type of neural network that is widely applied today owing to its effectiveness in solving almost all types of problems.

In [35,37], in order to classify fault types in electrical transmission systems, the variations in maximum coefficients from the first scale of a DWT extracted from high-frequency components at a duration of 1/4 cycle of phases A, B, C, and zero sequence of post-fault current signals, can be used as an input for the training process of an BPNN in a decision algorithm. Although the BPNN is very effective in classifying fault types, it cannot provide acceptable precision in classifying fault types in the loop structure of a transmission network. In fact, transmission lines are connected to each other and become a large grid-connected system owing to the increasing demand for electric power. During faults, it is necessary for the protection system to deal with a complicated transmission network. In practice, BPNN is partly limited by its slow training performance. In order to over-

come this problem, other neural network algorithms have been developed.

Therefore, this paper presents the development of a new decision algorithm used in the protective relays in order to classify faults in transmission systems. A transmission and distribution system in Thailand has been rapidly expanded and developed in a more complex manner along with economic and population growth. A newly developed algorithm and methodology to detect, identify, and classify faults in a system with fast response and accuracy are increasingly essential. A decision algorithm based on DWT and a probabilistic neural network (PNN) is investigated for inclusion in a transmission and distribution protection system.

The PNN was compared with the BPNN and the radial basis function (RBF) in a previous paper [37]. The obtained result from the PNN was more satisfactory and has less training time compared with the BPNN and RBF. The PNN was selected because it uses less training data and time compared with the BPNN and RBF. The fault conditions will be simulated using the Alternative Transients Program/Electromagnetic Transients Program (ATP/EMTP). ATP/EMTP is a universal programming system for the digital simulation of transient phenomena of an electromagnetic as well as electromechanical nature. Thus, ATP/EMTP is probably the most widely used power system transient program

in the world today. The analysis and diagnosis were performed using MATLAB on a PC Pentium IV at 2.4 GHz with 512 MB. The systems under consideration have a radial and loop overhead structure that includes a radial underground structure in order to show the advantage of the proposed method. Fault signals in each case are extracted to several scales on the DWT and are used as an input for a training process on the PNN. The validity of the proposed algorithm is tested with various fault inception angles, fault locations, and faulty phases. In addition, the construction of the decision algorithm is detailed and implemented with various case studies based on electricity transmission and distribution systems in Thailand. This includes the experimental set-up that was investigated in this paper.

2 Power system simulation using EMTP

ATP/EMTP is employed to simulate the fault signal transients at a sampling rate of 200 kHz (corresponding to the chosen sampling time used in ATP/EMTP, which is equal to 5 µs). The fault types are chosen based on Thailand's transmission and distribution system [36,41,42], as shown in Figs. 1, 2 and 3. In addition, a cross-sectional view of a cable is shown in Fig. 4. A transmission line with
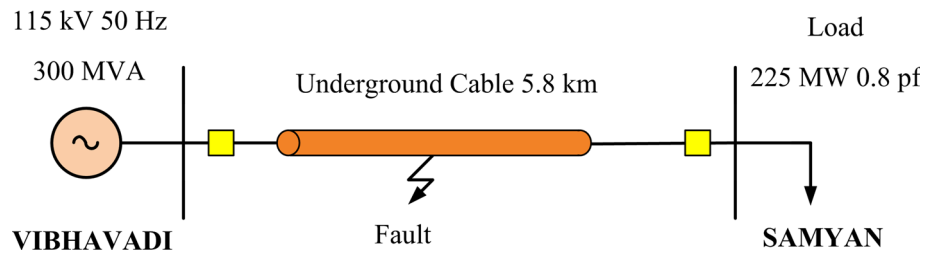

Fig. 1 System used in simulation studies for radial structure (System 1) [36,42]
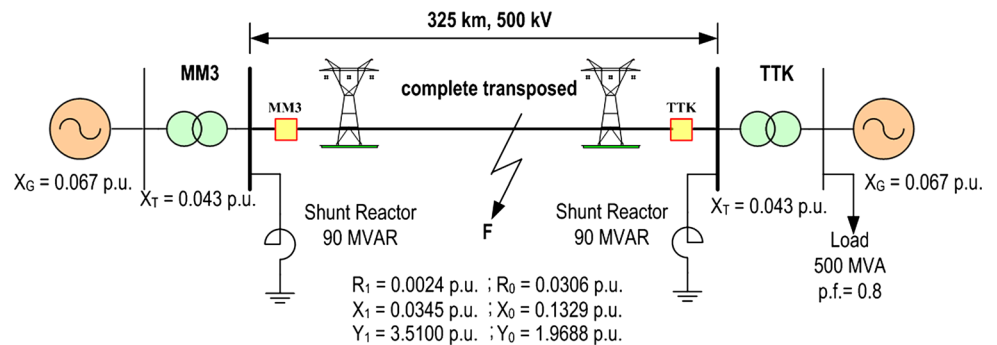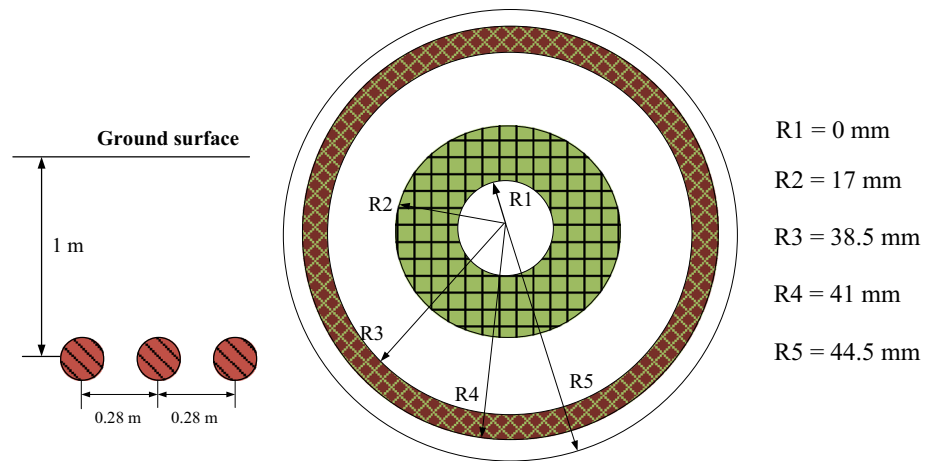

Fig. 2 System used in simulation studies for loop structure (System 2) [36,42]
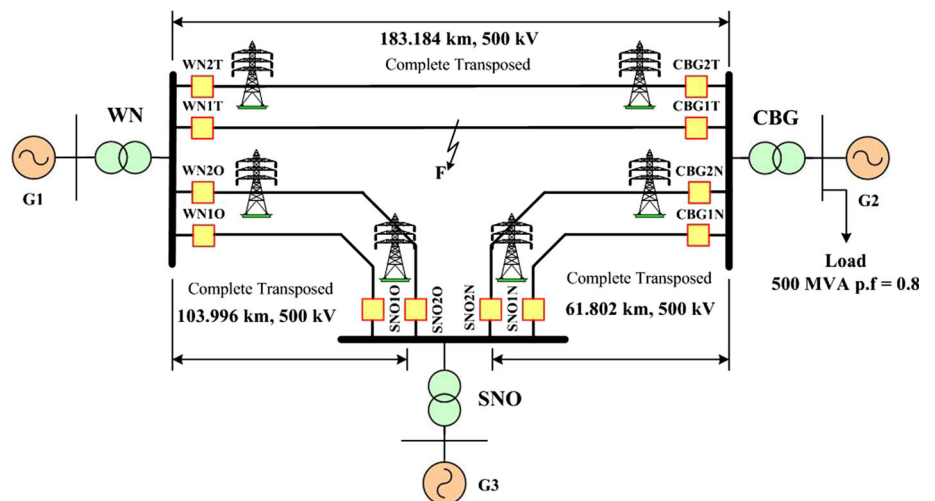
Fig. 3 System used in simulation studies for underground structure [41]

**Fig. 4** Configuration of cable in simulation studies [41]

R1 = 0 mm

R2 = 17 mm

R3 = 38.5 mm

R4 = 41 mm

R5 = 44.5 mm

Table 1 Number of various set and parameters for each set

Parameter of fault	Detail	Radial structure (System 1)	Loop structure (System 2)			Underground structure (System 3)
		MM3-TTK	WN-CBG	WN-SNO	SNO-CBG	VIBHAVADI-SAMYAN
Circuit of transmission system	Single circuit or double circuit	1	2	2	2	1
Angles of fault inception	0°–330° (each step is 30°), and phase A voltage is reference	12	12	12	12	12
Type of fault	Single line to ground, double lines to ground, line to line, and three phase	10	10	10	10	10
Fault location for overhead transmission line	Distances of 10, 20, 30, 40, 50, 60, 70, 80, and 90%, measured from the sending end	9	9	9	9	–
Fault location for underground distribution cable	The distance of 1–5 km (each step = 1 km) of the underground cable length measured from the sending end	–	–	–	–	5
Fault resistance	10 Ω	1	1	1	1	1
Total		1080	2160	2160	2160	600

frequency-dependent parameters can be calculated by supporting routing line cable constants (LCC) in ATP/EMTP. The LCC model is based on the geometrical and material data for an overhead line and underground cable, including the corresponding electrical data. Simulations were performed with various changes in system parameters, as shown in Table 1. The fault signals generated using ATP/EMTP were interfaced to MATLAB in order to analyse the transient high-frequency components by using a wavelet toolbox.
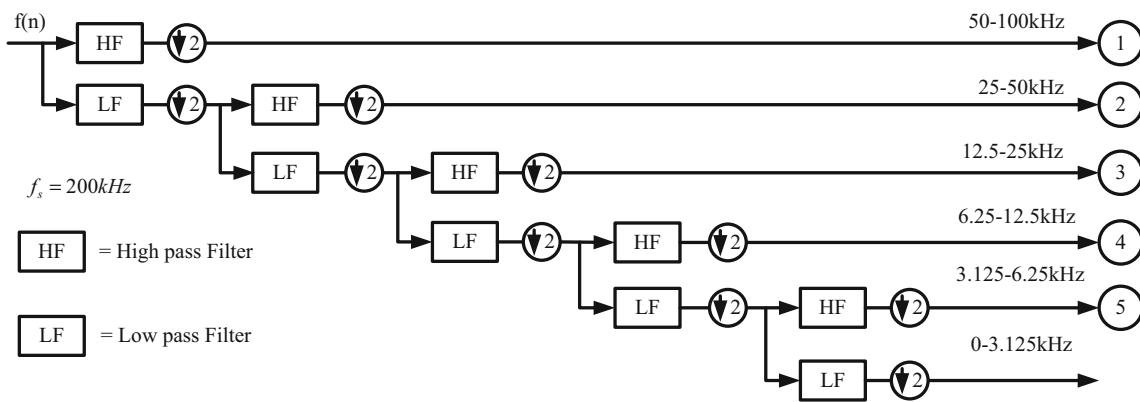
Fig. 5 Five-level wavelet decomposition tree

Fig. 6 Example of DWT from scale of 1–5 for positive sequence of phase A to ground fault in transmission system (section MM3-TTK)
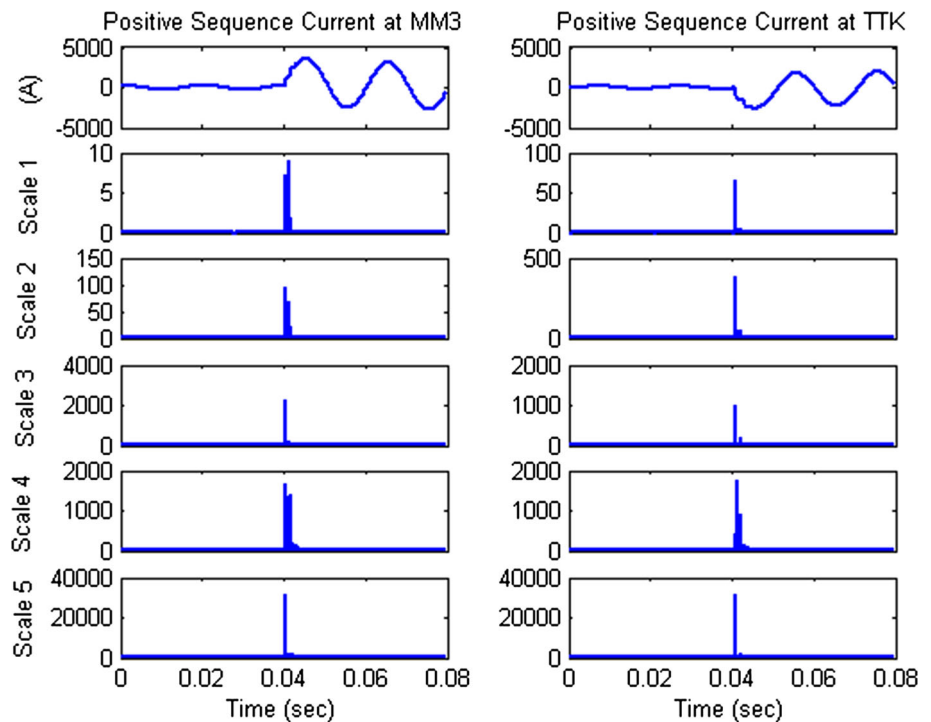

3 Fault detection decision algorithm

After simulating the fault signals, a fault detection decision algorithm [19,35–37] is processed using the positive sequence current signals. A Clarke transformation matrix [19] was used to calculate the positive sequence and the zero sequence of the current. The fault signals generated using ATP/EMTP are extracted to several scales using the mother wavelet daubechies4 (db4) [19,37,43–45] of the DWT in order to decompose high-frequency components, as shown in Fig. 5. The daubechies (db) was chosen as the mother wavelet in this paper because according to the literature [37,44,45], the daubechies mother wavelets are widely used for analysing signals in power systems. Moreover, after testing many mother wavelets, the daubechies4 (db4) seemed

to be satisfactory in acquiring reasonable accuracy in fault classification.

By considering Fig. 5, the original input signal is split into five scales by analysing the high frequencies called details (high-pass portion). For each stage (scale 1, …, scale 5), the filters have different cut-off frequencies and bandwidths, while the processed signal remains unchanged. The frequency bandwidth of the level's band decreases as the level scale increases. This implies that the frequency resolution increases as the level scale increases. In addition, the coefficients of signals obtained using DWT, then, are squared so that abrupt changes in the spectra can be clearly found. This is illustrated in Figs. 6 and 7.

An example of a DWT for a radial structure is illustrated in Fig. 6. This is phase A to ground fault (AG) at 35% of
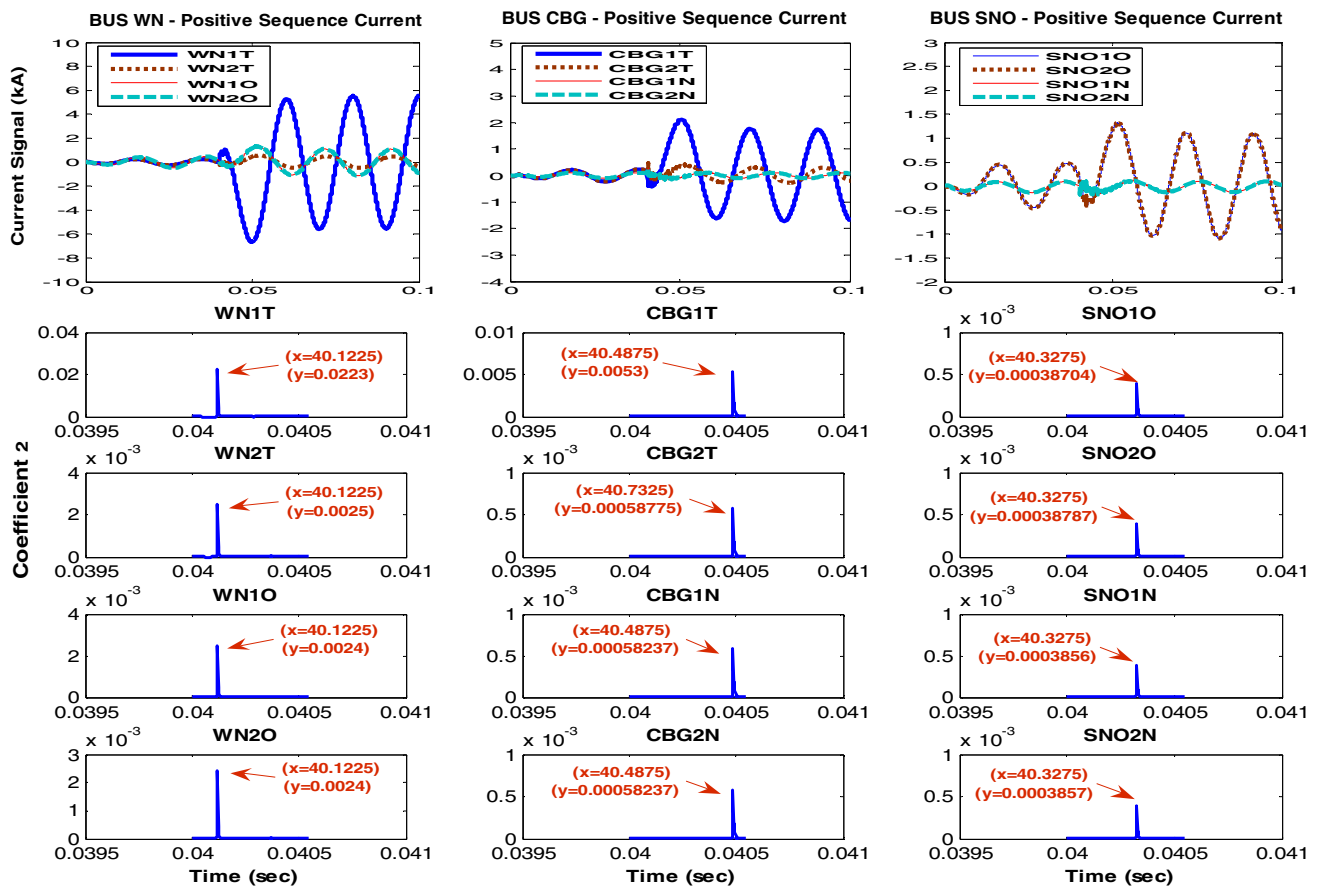
Fig. 7 Example of DWT from scale 1 for the positive sequence of phase A to ground fault in the transmission system (section WN-CBG) [45], where, WN1T and WN2T are WN bus section WN-CBG circuit 1 and circuit 2, respectively. WN1O and WN2O are WN bus section WN-SNO circuit 1 and circuit 2, respectively. CBG1T and CBG2T are CBG bus section WN-CBG circuit 1 and circuit 2, respectively. CBG1N and CBG2N are CBG bus section SNO-CBG circuit 1 and circuit 2, respectively. SNO1O and SNO2O are SNO bus section WN-SNO circuit 1 and circuit 2, respectively. SNO1N and SNO2N are SNO bus section SNO-CBG circuit 1 and circuit 2, respectively.

the length of section MM3-TTK in the transmission network shown in Fig. 1. By considering Fig. 6, the input signal implementation is a multisignal trace from each high-pass filter corresponding to a particular scale parameter. The traces labelled scale 1, scale 2, …, scale 5 in this figure correspond to the filter output of Fig. 5. In addition, by observing Fig. 6, during the prefault condition, the coefficient detail at each scale of the DWT obtained from the positive sequence current is treated as zero. After a fault occurrence at 0.04 s, during the post-fault condition, the coefficient detail at each scale of the DWT obtained from the positive sequence current has a sudden change compared with those before the occurrence of the fault, and this change plays an important role in the fault detection decision algorithm. This indicates that the fault detection decision algorithm can be beneficial. Therefore, the result obtained from the fault detection algorithm presumes that these signals are in their fault conditions.

Similarly, by observing Fig. 7, this is a phase A to ground fault (AG) at 20% of the length of section WN-CBG in the transmission network shown in Fig. 2. Owing to the loop structure of the transmission network, there are changes in phase–phase current waveshapes at all buses of the network (WN, CBG, and SNO). According to the behaviour presented in Figs. 6 and 7, the similarity between the behaviours of the coefficient details of the DWT can be clearly seen. This indicates that the fault detection decision algorithm can benefit from variations in the coefficient. Based on a further analysis of Fig. 7, the coefficient detail from scale 1 of the DWT does change. Therefore, the result obtained from the fault detection algorithm presumes that these signals are in their fault conditions. However, when carefully considering Fig. 7, it is found that all coefficients obtained from the positive sequence currents at every bus have a change of more than five times the normal value during the faults owing to the effect of the loop structure of the transmission network. As a result, the fault detection algorithm fails with a comparison of coefficients when dealing with a loop (double-circuit or multiterminal) transmission line, but the algorithm gives sat-

isfactory results for a radial (single-circuit or two-terminal) transmission line. In order to overcome this problem, a new fault detection algorithm has been developed so that the effect of the loop structure can be included.

After applying the DWT to positive sequence current, a comparison of the coefficient details from each scale is considered. A comparison between the maximum coefficients in the first scale of each bus, which can detect faults, is made in order to detect the faulty bus. From Fig. 7, it can be seen that maximum coefficients of positive currents from the faulty buses involving a fault location (in this case, WN1T and CBG1T, with the fault location between them) have the highest values when compared with those of other healthy buses. For the improvement fault detection algorithm, in the case of a double-circuit or multiterminal system, the maximum coefficients obtained from the same buses are also compared in order to detect the faulty circuit as follows:

If $\text{WN1T}^L_{(post)} > \max\left(\text{WN2T}^L_{(post)}, \text{WN1O}^L_{(post)}, \text{WN2O}^L_{(post)}\right)$
then RELAY WN1T TRIP
elseif $\text{WN2T}^L_{(post)} > \max\left(\text{WN1T}^L_{(post)}, \text{WN1O}^L_{(post)}, \text{WN2O}^L_{(post)}\right)$
then RELAY WN2T TRIP
elseif $\text{WN1O}^L_{(post)} > \max\left(\text{WN1T}^L_{(post)}, \text{WN2T}^L_{(post)}, \text{WN2O}^L_{(post)}\right)$
then RELAY WN1O TRIP
elseif $\text{WN2O}^L_{(post)} > \max\left(\text{WN1T}^L_{(post)}, \text{WN2T}^L_{(post)}, \text{WN1O}^L_{(post)}\right)$
then RELAY WN2O TRIP
end

where $L =$ the scale of DWT.

After the fault detection process, the maximum coefficient of the phase A, B, C, and zero sequence currents obtained from the faulty bus is used as an input for the training process of the PNN.

4 Neural network decision algorithm and simulation results

After the fault detection process, the coefficient details of scale 1, which are obtained using the DWT, are used for training and test processes of the PNN [46,47]. By considering the data in Table 2, the input data sets are 720, 4320, and 300 for

training the radial structure, loop structure, and underground structure, respectively. There are 360, 2160, and 150 sets for the validation radial structure, loop structure, and underground structure, respectively. Before the training process, the PNN structure consists of four neurons (input) and one neuron (output), whereas the number of neurons in the radial basis layer is always equal to the number of training sets. The input patterns are maximum coefficients of the DWT at 1/4 cycle of phase A, B, C, and zero sequence for post-fault current waveforms, as shown in Fig. 8. The output variables of the PNN are designated in a range of 1–10, corresponding to various types of fault, as shown in Table 3.

Figure 9 shows an algorithm used in the training process for the PNN. The maximum coefficient details of the DWT (input variables, as shown in Fig. 8; and the output variable, as shown in Table 2) are used to prepare the data by normalization because the obtained data will clearly analyse the pattern. The obtained data are propagated to each neuron in the radial basis layer. During the training process, PNN begins with a random initial weight and increasing spread in the radial basis layer, which corresponds to the bias value $(b = \frac{0.8326}{\text{Spread}})$ from 0.0001 until 0.1. For each iteration, the radial basis layer computes distances from the input vector to the weight vector and produces an output in the radial basis layer based on Eq. 1 [36,47]:

$$\varphi(p) = \exp\left(-\frac{\left\|p - \text{IW}_{1,1}\right\|^2}{\sigma_j^2}\right) \tag{1}$$

where $p =$ input pattern vector, $\text{IW}_{1,1} =$ centre vector of radial basis layer, $\sigma =$ spread constant for radial basis layer (smoothing parameter), $\varphi(p) =$ output of radial basis layer.

After the output of the radial basis layer is determined, each neuron in the competitive layer receives all the radial basis layer outputs that are associated with a given class and produces a net output that consists of a vector of probabilities. Finally, a competitive activation function applied to the output of the competitive layer determines the maximum of these probabilities and produces a value of 1 for that class and 0 for the other classes, as in Eq. 2 [46]:

$$o/p_{\text{ANN}} = f^2\left(\text{LW}_{2,1} \times \varphi(p)\right) \tag{2}$$

Table 2 Number of data for decision algorithm

Number of set	Radial structure (System 1)	Loop structure (System 2)			Underground structure (System 3)
	MM3-TTK	WN-CBG	WN-SNO	SNO-CBG	VIBHAVADI-SAMYAN
Training	720	1440	1440	1440	300
Validation	360	720	720	720	150
Case studies	360	720	720	720	150
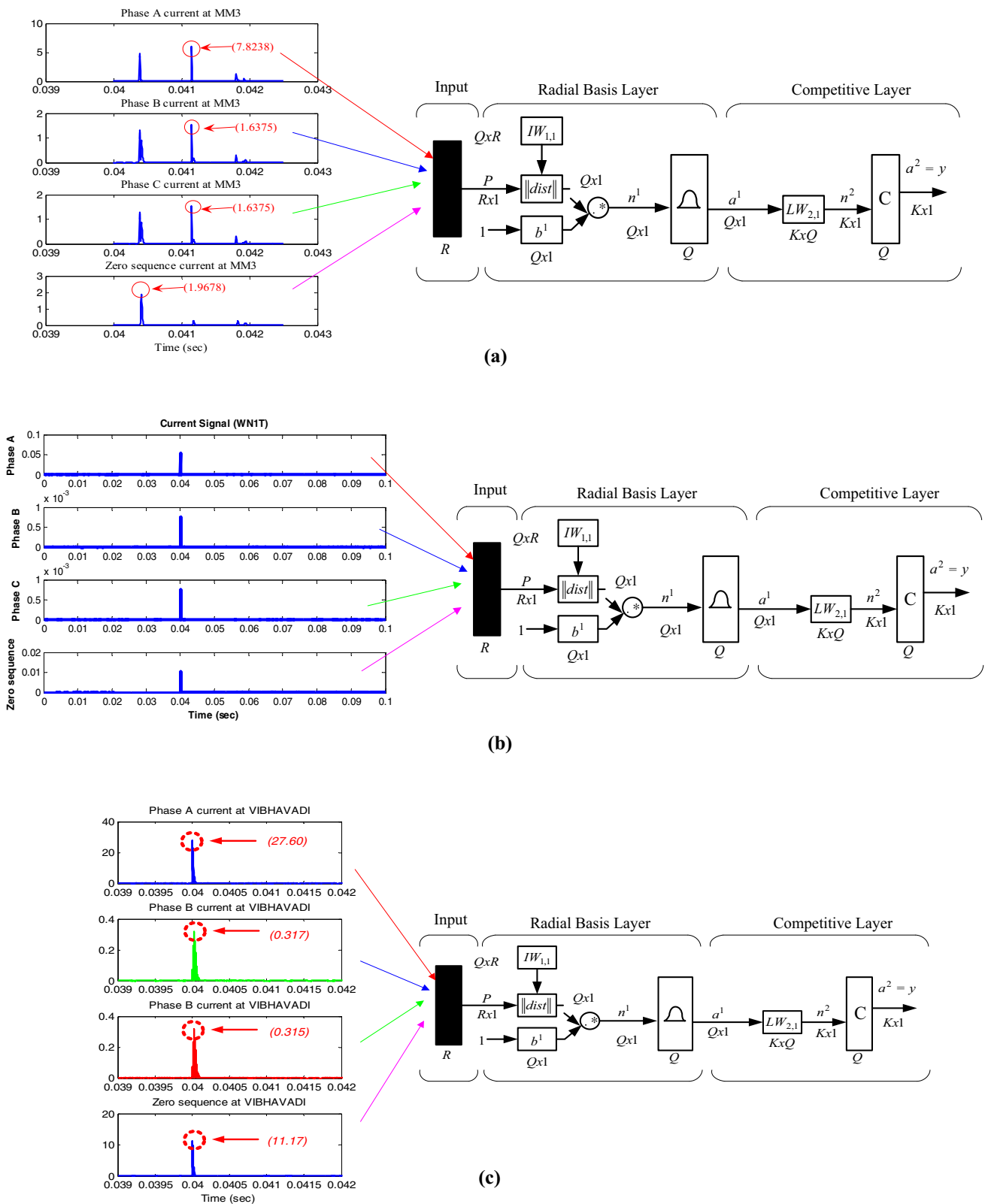
Fig. 8 Magnitude in scale 1 for post-fault current signal. **a** Post-fault current signal in radial structure (section MM3-TTK), **b** post-fault current signal in loop structure (section WN1T-CBG1T), **c** post-fault current signal in underground structure (section VIBHAVADI-SAMYAN)

Table 3 Output patterns from neural networks

Output of PNN	Classification of fault type	Types of fault
1	Phase A to ground fault	AG
2	Phase B to ground fault	BG
3	Phase C to ground fault	CG
4	Phase A, B to ground fault	ABG
5	Phase B, C to ground fault	CAG
6	Phase C, A to ground fault	BCG
7	Three-phase fault	ABC
8	Phase A to phase B fault	AB
9	Phase C to phase A fault	CA
10	Phase B to phase C fault	BC

where f^2 = competitive activation function, $LW_{2,1}$ = weight vector between radial basis layer and competitive layer.

After computing the output of the PNN for each iteration, the number of errors in the test sets can be calculated to be used as an index for efficiency determination of the PNN. If the number of errors is zero, then the weight and bias will be collected and verified with case study sets after the training process. If the number of errors is more than zero, then the weight and bias will be improved, and its output will try to match the target output in the next iteration.

For the next iteration, a step spread increase of 0.0001 is used to compute the number of minimum errors again. This procedure is repeated until the maximum number of spreads is reached, or the number of minimum errors of the test set is zero. Then, training will be stopped. The training process is summarized in a flowchart in Fig. 9. Results from the training process are listed in Table 4.

The BPNN is compared with the proposed decision algorithm in order to show the benefits of the proposed decision algorithm. Before the BPNN training process [35], a structure of the BPNN consists of four neuron inputs in the input layer, two hidden layers, and one neuron output in the output layer. The initial and final number of neurons for the first hidden layer are two and 11 neurons, respectively. During the training process [35], the weight and biases are adjusted to compute the mean absolute percentage error (MAPE). The MAPE is an index to determine the efficiency of the BPNN. The training procedure was stopped when the final number of neurons for the first hidden layer was reached, or when the MAPE of the validation sets was less than 0.5%. Results from the training process are listed in Table 4. Based on the training times in Table 4, the PNN has less training time than the BPNN.

After the training process, the algorithm was employed to classify fault types in the transmission systems. Case studies were varied to verify the algorithm's capabilities. The system under consideration is shown in Figs. 1, 2 and 3. Various
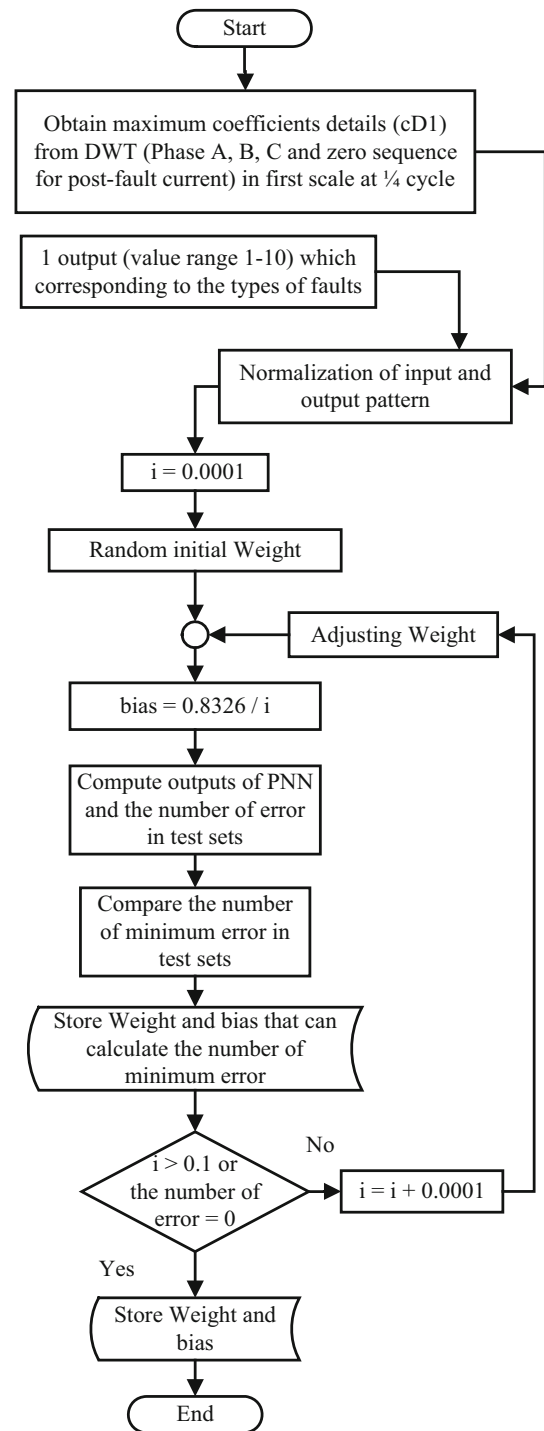

Fig. 9 Flowchart for training process

case studies were performed with various types of faults at each location on the transmission and distribution network, including variations in fault inception angles and locations on each transmission and distribution line. The total number of case studies for the radial structure, loop structure, and underground structure was 360, 2160, and 300 sets, respectively.

Table 4 Comparison of results of training process

| Information for comparison	Radial structure		Loop structure		Underground structure	
	BPNN	PNN	BPNN	PNN	BPNN	PNN
Number of neurons input	4	4	4	4	4	4
Number of neurons in hidden 1 for BPNN (or radial basis layer for PNN)	11	611	11	3456	11	300
Number of neurons in hidden 2	10	–	10	–	10	–
Spread	–	0.0022	–	0.002	–	0.001
Number of neurons output	1	1	1	1	1	1
Iterations	20,000	611	20,000	3456	20,000	300
Total time of training process (min)	20	1	160	9.708	35	1
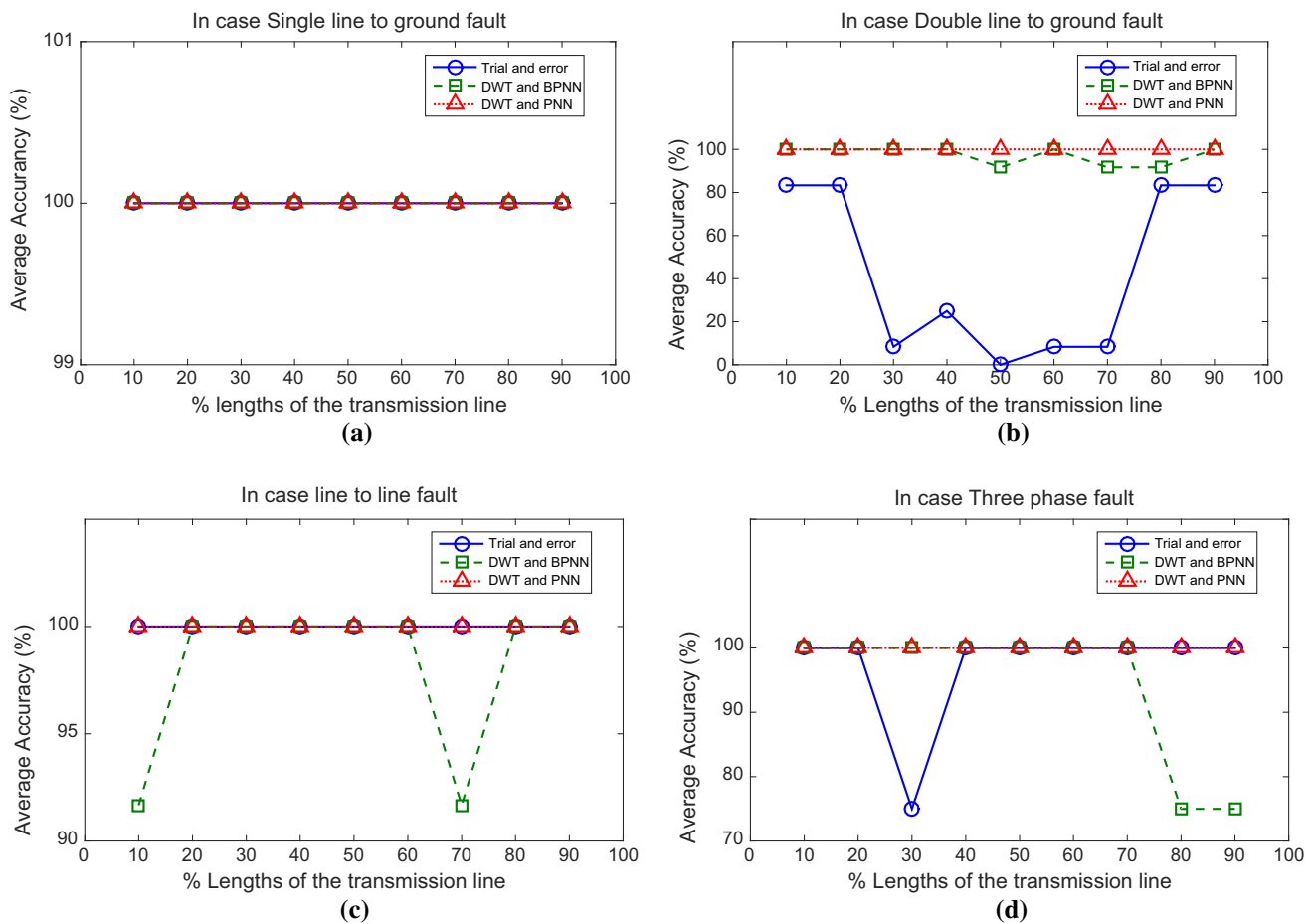
Fig. 10 Comparison of average accuracy of fault classification for various lengths of transmission line system 1 where fault occurs. **a** Case of single line-to-ground fault (SLG), **b** case of double line-to-ground fault (DLG), **c** case of line-to-line fault (L–L), **d** case of three-phase fault (3-P)

Figures 10, 11 and 12 and Table 5 show a comparison of the average accuracy between the decision algorithm using PNN, decision algorithm using BPNN, and decision algorithm using a comparison of the coefficients of the DWT or trial and error that was developed by Markming et al. [19].

Based on a further analysis of Figs. 10, 11 and 12, it can be observed that the obtained average accuracy from the decision algorithm also gives better results than the other techniques [19] at various lengths of the transmission lines in which faults occur. The proposed decision algorithm gives better results than the other algorithms [19,35]. The trial-and-error technique gives satisfactory results with both structures but not in the case of a double line-to-ground fault. In Figs. 10b and 11b, when the double line-to-ground fault
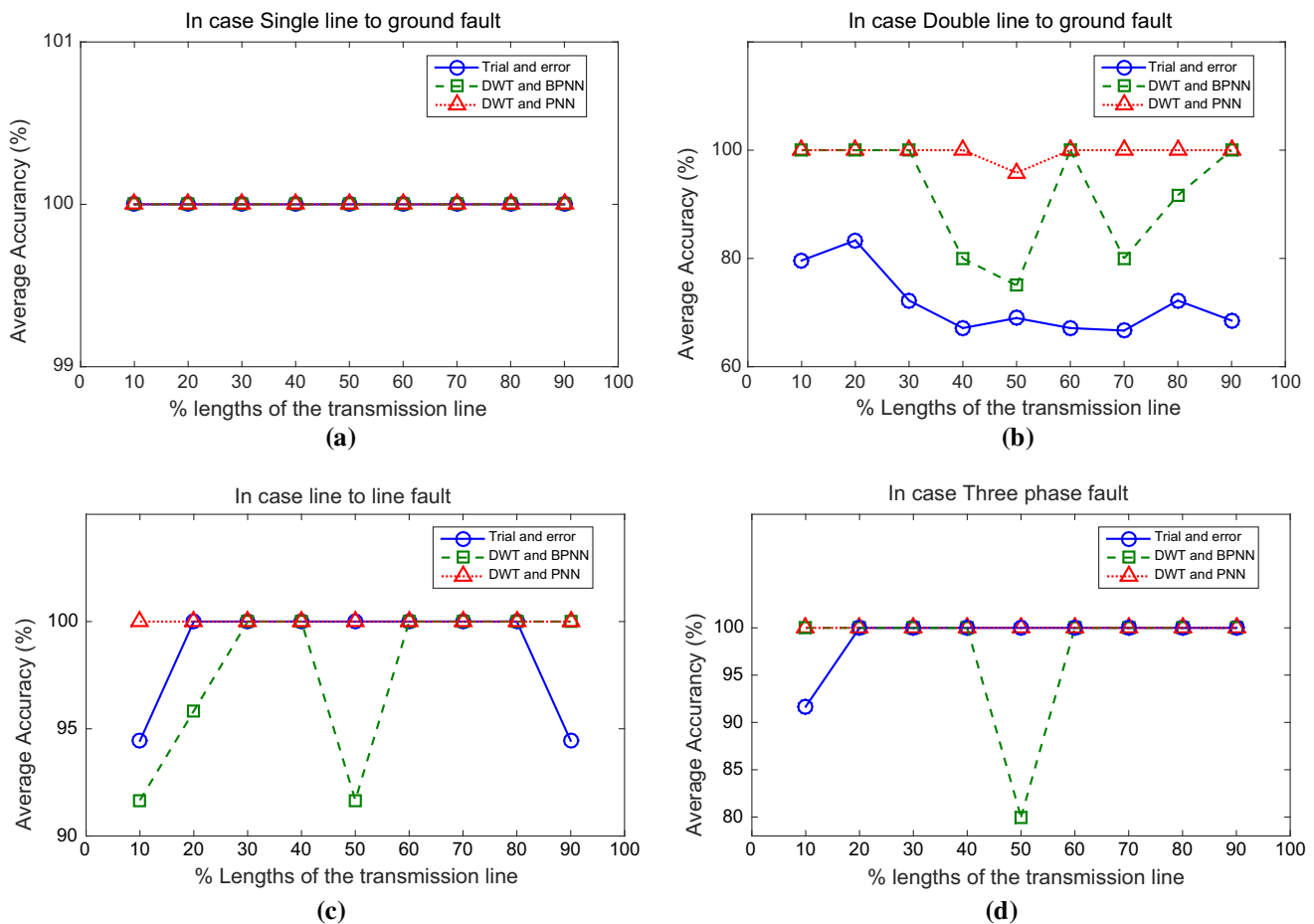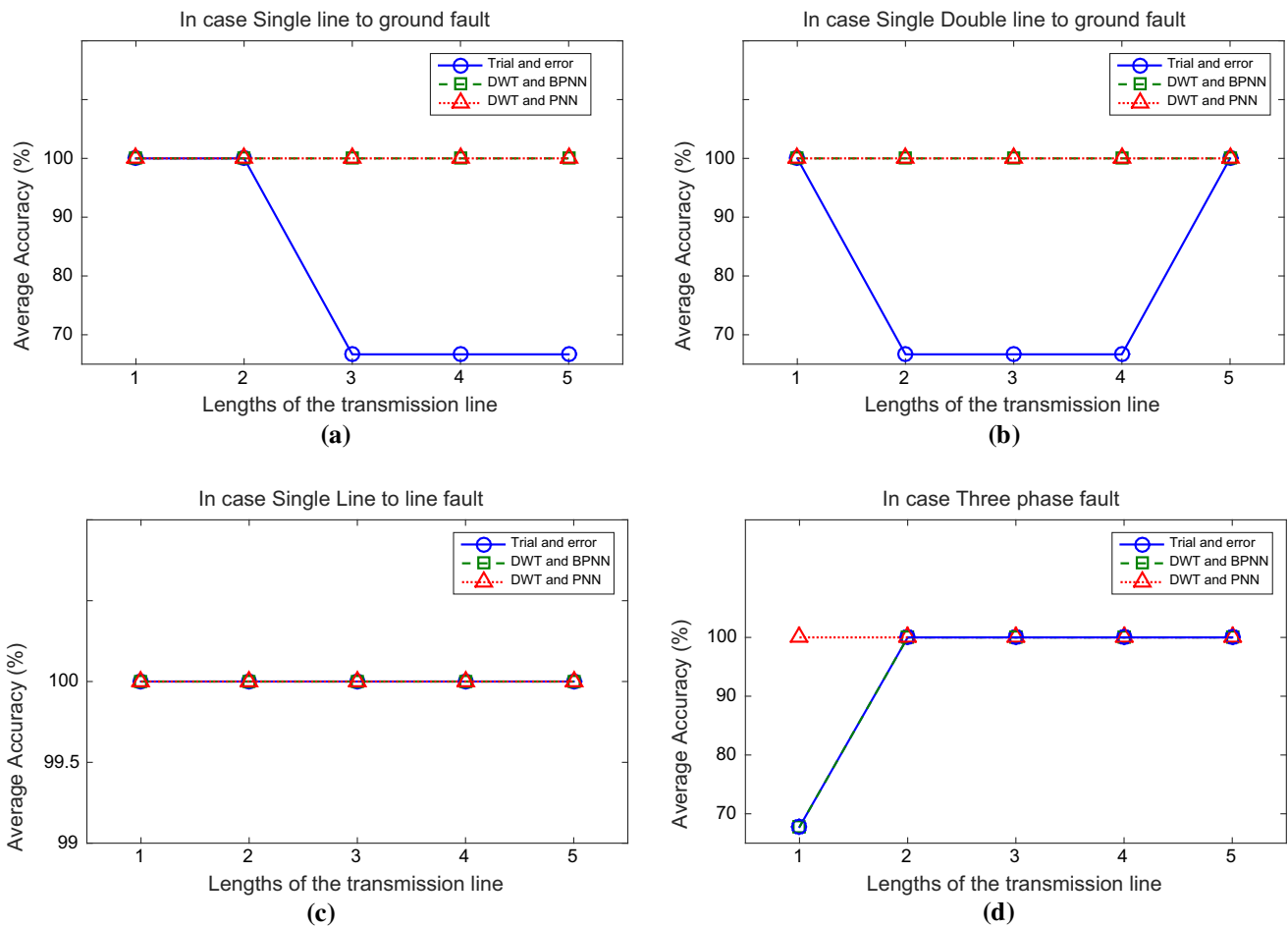
Fig. 11 Comparison of average accuracy of fault classification for various lengths of transmission lines (System 2) where fault occurs. **a** Case of single line-to-ground fault (SLG), **b** case of double line-to-ground fault (DLG), **c** case of line-to-line fault (L–L), **d** case of three-phase fault (3-P)

occurring between 30 and 70% of the length measured from the sending end is considered, it can be observed that the obtained average accuracy from the trial-and-error technique has an unacceptable precision in classifying the fault types, as shown in Fig. 10b. On the other hand, the proposed algorithm is unaffected for the fault classification for a double line-to-ground fault between 30 and 70% of the length measured from the sending end. This indicates that the proposed decision algorithm can classify the various types of fault for radial and loop structures.

Table 5 shows the average accuracy for fault classification for each structure as obtained from the proposed decision algorithm, BPNN algorithm, and trial-and-error technique. This shows the advantage of the PNN algorithm when dealing with a loop-structure transmission network. As a result, the obtained results for both structures have little impact on the average accuracy. It can be concluded that the proposed algorithm can classify the types of fault in the transmission and distribution system with an accuracy of higher than 99%.

5 Experiment results for fault detection and classification

The section of MM3-TTK transmission system is modelled and developed on an experimental bench in a laboratory environment in order to verify the model used in the simulation. Then, the proposed algorithm detection and classification of fault signals is applied to an actual system. The overall experimental set-up in the laboratory is shown in Fig. 13. By considering Fig. 13a, the variable voltage transformer was employed to adjust the voltage level of the experimental set-up at 400 V_{LL} from the laboratory's supply at point No. 1, as shown in Fig. 13a. The circuit breakers and fuses at point No. 2 were employed as protective devices to prevent damage to the supply. Then, the electric parameters at the source side (sending end) and load side (receiving end)—such as voltage, current, and real power including the power factor—can be achieved with the power meter at points Nos. 3 and 4 in Fig. 13a, respectively.

Fig. 12 Comparison of average accuracy of fault classification for various lengths of underground distribution lines (System 3) where fault occurs. **a** Case of single line-to-ground fault (SLG), **b** case of double line-to-ground fault (DLG), **c** case of line-to-line fault (L–L), **d** case of three-phase fault (3-P)

The transmission line model was designed with a π model. By considering Fig. 13b, the inductor and capacitor were used in the transmission line model. Fifteen inductors of 120 mH and the six inductors of 60 mH were connected in series to obtain the desired value. In addition, the 0.1-μF capacitors at a rated voltage of 400 V_{AC} were also connected in parallel or in series to obtain the desired values. An incandescent lamp (resistance load) was used as a linear load, whereas the magnetic ballast (inductance load) including the incandescent lamp were used as a nonlinear load.

A comparison between results from the ATP/EMTP simulation program and the experimental set-up was conducted in order to evaluate the correctness of the simulation model and parameter data. Figure 14a, b shows current signals obtained from the experimental set-up and ATP/EMTP program, respectively. The case study in the figure is a single line-to-ground fault at a distance of 30% along the transmission line from the substation bus, and the fault angle is 180°

of the phase A waveform. Figures 15, 16 and 17 also show a comparison between the simulation and the experimental set-up using the same parameter settings as the case study in Fig. 14, but using various fault types. Figure 15 shows an example case study of a double line-to-ground fault. Figure 16 shows an example case study for a line-to-line fault. Figure 17 shows an example case study of a double line-to-ground fault. This indicates that the results of the simulation model of the fault in a transmission line align with the results from the experimental set-up in all case studies. Thus, it can be concluded that the simulation model and data can be applied to an actual system.

The fault signals generated using the experimental set-up are extracted to several scales with the daubechies4, as shown in Figs. 18 and 19. By considering the coefficients obtained using a DWT, it is seen that when a fault occurs, the coefficients of high-frequency components have a sudden change compared with those before a fault occurs. Therefore, the result obtained from the fault detection algorithm presumes

Table 5 Comparison of average accuracy for fault classification for various types of faults at each location on the transmission network

| Section	Types of faults	Number of case studies	Fault detection (%)	Average accuracy (%)		
				Trial-and-error method [19]	DWT and BPNN [35]	DWT and PNN
MM3-TTK	SLG	108	100	100.00	100.00	100.00
	DLG	108	100	42.59	97.22	100.00
	L–L	108	100	100.00	98.15	100.00
	ABC	36	100	97.22	94.44	100.00
WN-CBG	SLG	216	100	100.00	100.00	100.00
	DLG	216	100	72.22	92.59	100.00
	L–L	216	100	100.00	98.14	100.00
	ABC	72	100	100.00	98.61	100.00
WN-SNO	SLG	216	100	100.00	100.00	100.00
	DLG	216	100	72.22	91.67	100.00
	L–L	216	100	100.00	97.68	100.00
	ABC	72	100	100.00	97.22	100.00
SNO-CBG	SLG	216	100	100.00	100.00	100.00
	DLG	216	100	70.83	88.89	98.61
	L–L	216	100	96.29	97.22	100.00
	ABC	72	100	100.00	97.22	100.00
Underground	SLG	45	100	80.00	100.00	100.00
	DLG	45	100	80.00	100.00	100.00
	L–L	45	100	100.00	100.00	100.00
	ABC	15	100	100.00	93.33	93.33
Average		2670	100	90.71	96.78	99.85

that these signals are in their fault condition. However, signals obtained from the actual experimental set-up consist of noise, especially after entering the steady state of a fault signal. The reason is that an actual experimental set-up has some factors that can affect the signal measurement process. Thus, the amplitude of the fault current can amplify a noise signal when applied to signal processing. A noise signal from an experimental set-up does not affect fault detection or a classification algorithm because the wavelet coefficient when a fault occurs is higher than that of other states. For the next step, the maximum coefficient details from the variations in the first-scale high-frequency components that can detect faults of phase A, B, C, and zero sequence of post-fault current signals obtained by the DWT are also verified for their decision algorithm capability. This is done with a decision algorithm using PNN, a decision algorithm using BPNN [35], and a decision algorithm using trial and error [19]. The results show that the proposed algorithm can classify types of fault with an average accuracy of higher than 90%, as shown in Table 6.

Table 6 lists the fault classification accuracies of various algorithms, and a comparison between proposed methods and previous methods in past research studies. From the table, it can be seen that the proposed method can achieve satisfactory results when classifying faults with an average accuracy of higher than 90%, when compared with algorithms proposed in previous research studies.

6 Conclusions

This paper proposed an algorithm based on a combination of DWT and PNN algorithms to classify types of faults in transmission and distribution systems. The radial structure and loop structure of transmission systems, and the radial underground structure of distribution systems, are investigated to verify their algorithm capability. Daubechies4 (db4) was selected as a mother wavelet to decompose high-frequency components from fault signals. Positive sequence current signals were used in fault detection. The maximum coefficient details from the variations in first-scale high-frequency components that can detect faults at 1/4 cycle of phase A, B, C, and zero sequence of post-fault current signals obtained by the DWT were used as inputs for the training process of a PNN in a decision algorithm. The results show that the proposed algorithm is able to detect a faulty bus with an accuracy of 100%, and classify types of fault with an average accuracy of higher than 99%.

(a)

(b)

(c)
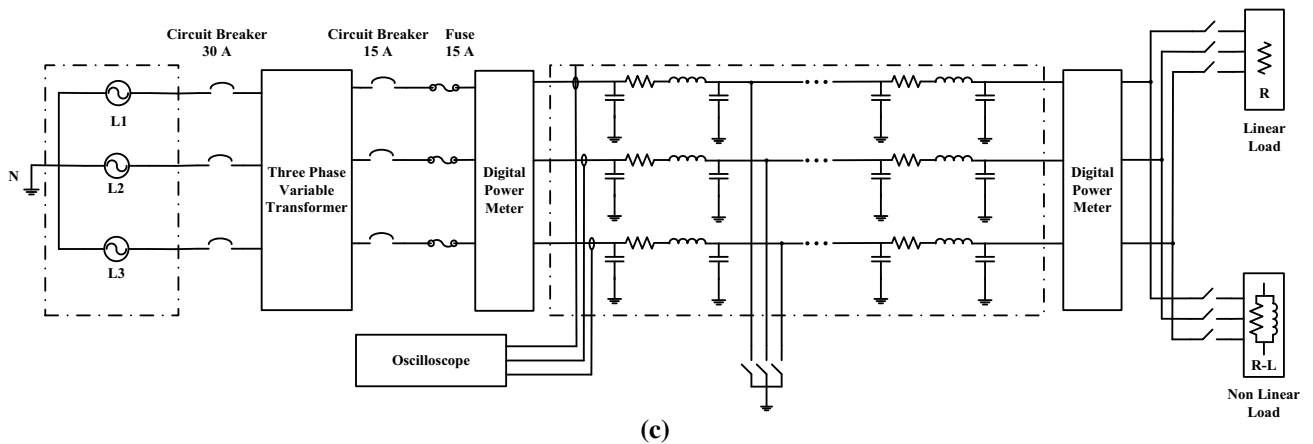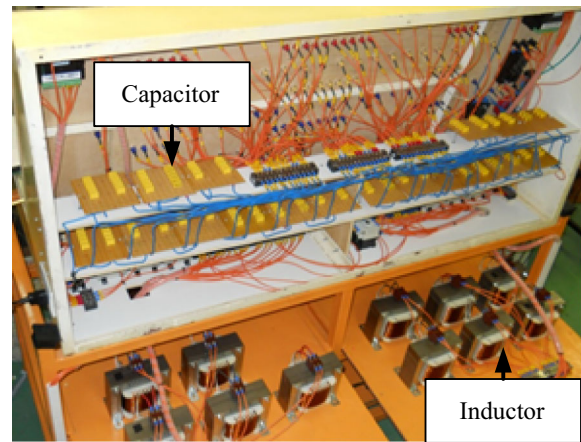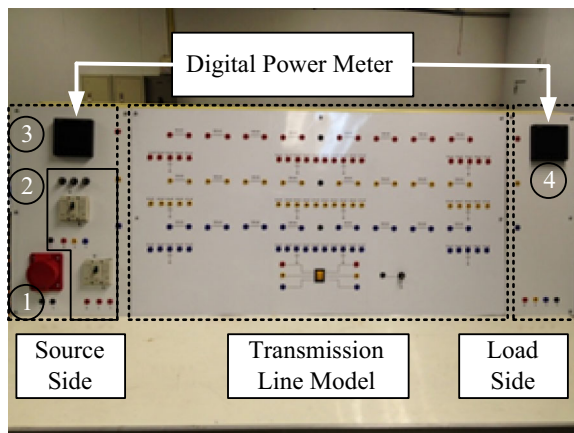
Fig. 13 Experimental set-up for fault signal generation in transmission system. **a** In front of the experimental set-up, **b** capacitor and inductor of the experimental set-up, **c** single-line diagram
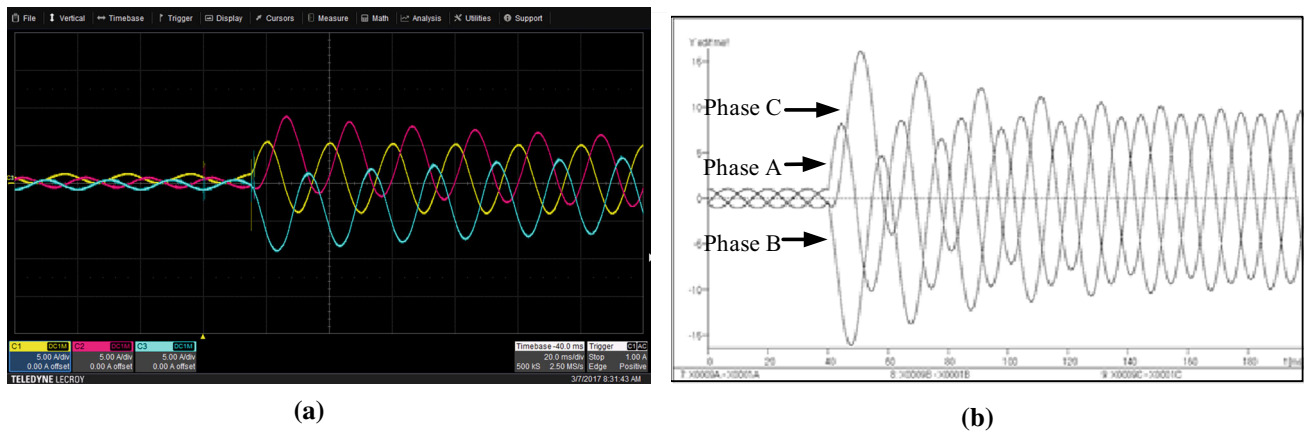

(a)

(b)
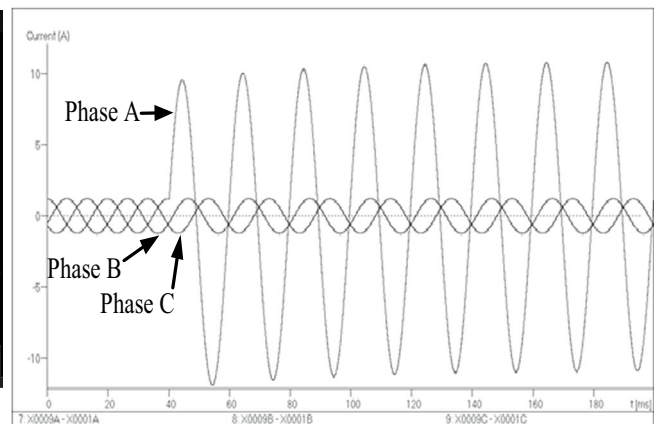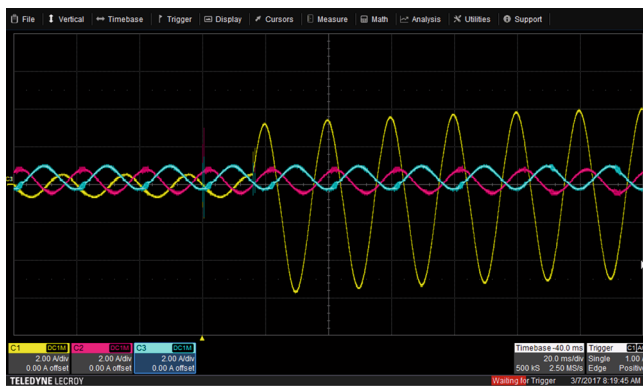
Fig. 14 Example of current signal for single line-to-ground fault. **a** Experimental set-up, **b** ATP/EMTP program
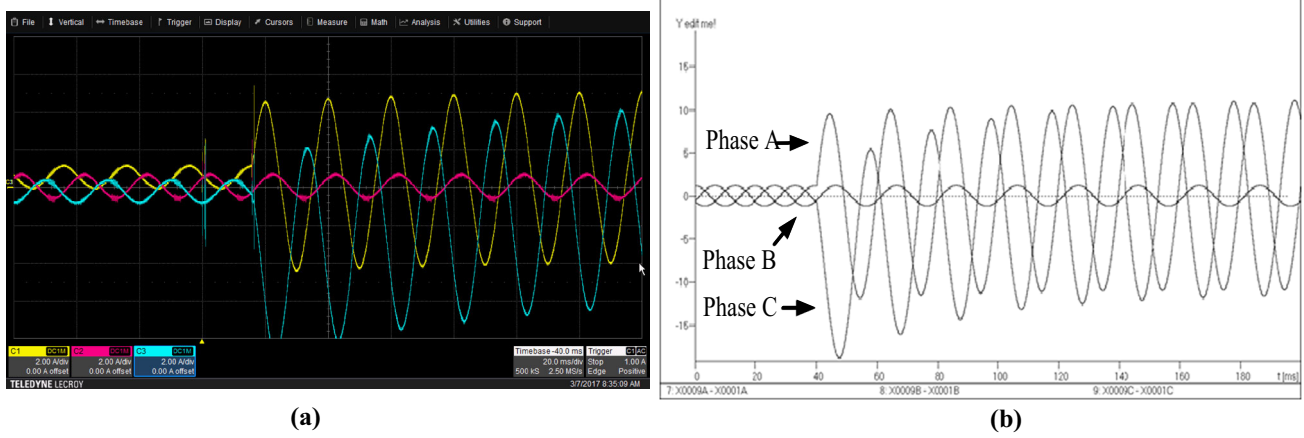
Fig. 15 Example of current signal for double line-to-ground fault. **a** Experimental set-up, **b** ATP/EMTP program
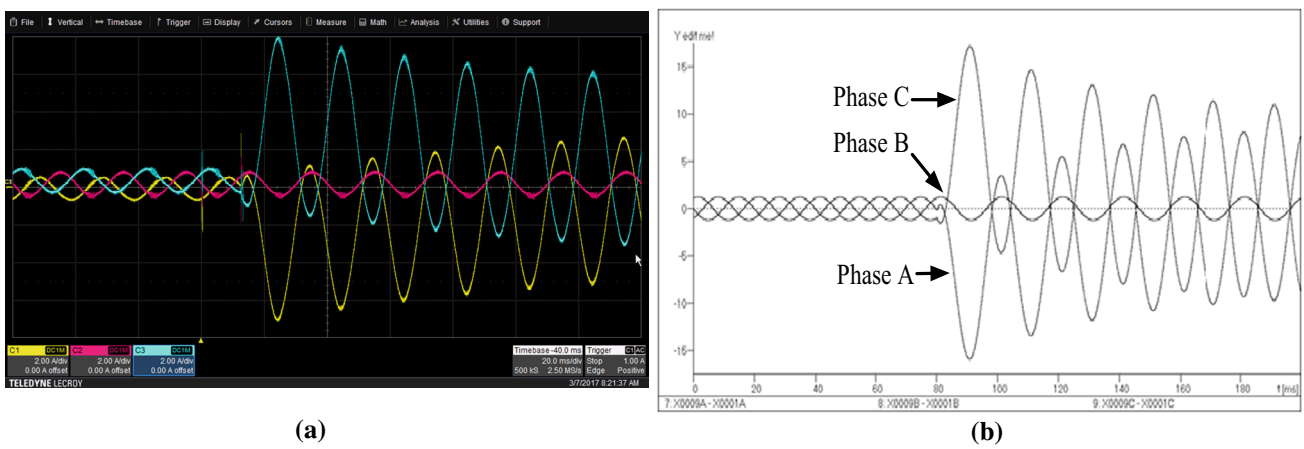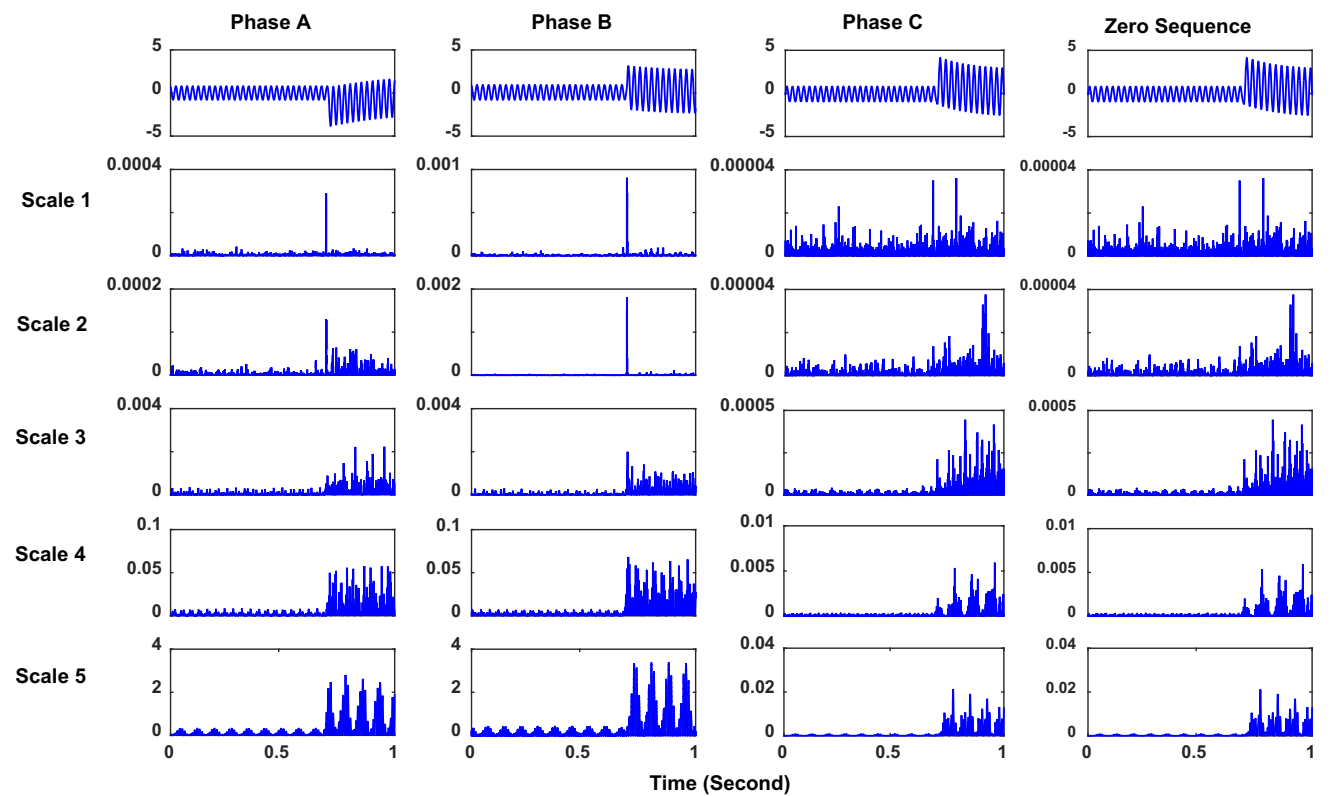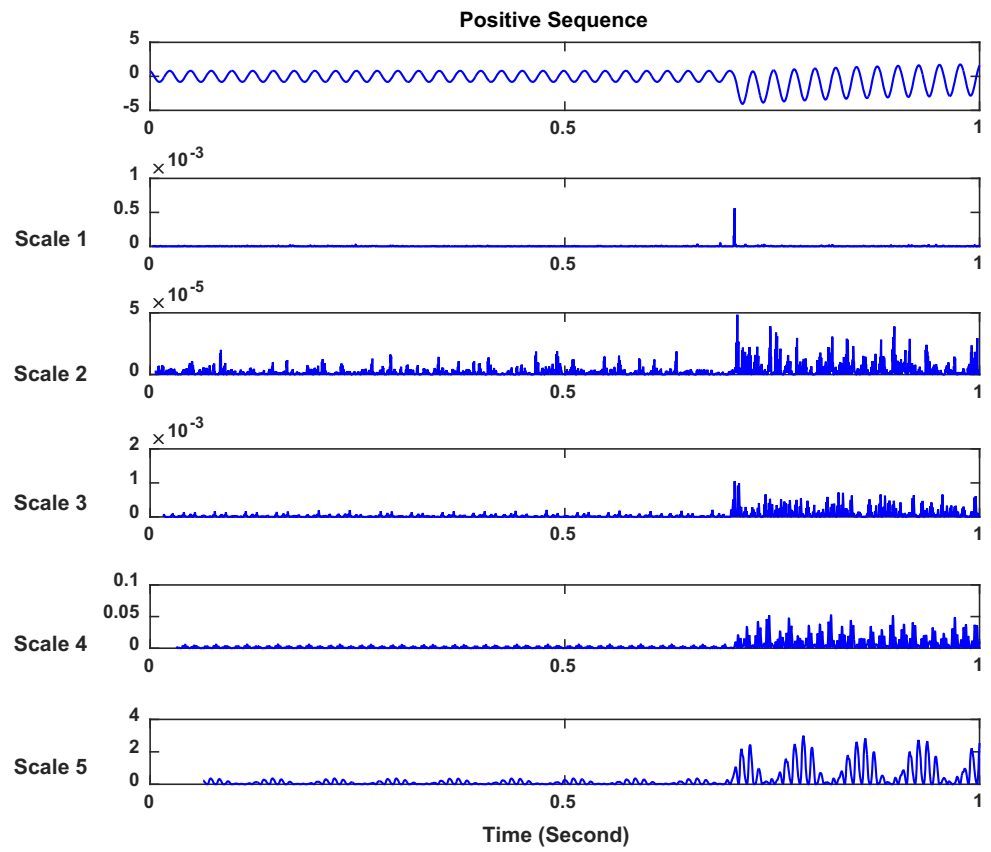

Fig. 16 Example of current signal for line-to-line fault. **a** Experimental set-up, **b** ATP/EMTP program

Fig. 17 Example of current signal for three-phase fault. **a** Experiment set-up, **b** ATP/EMTP program

Fig. 18 Example of DWT from scale of 1–5 for positive sequence of three-phase fault in the experimental set-up

Fig. 19 Example of DWT from scale of 1–5 for the phase A, phase B, phase C, and Zero sequence of three-phase fault in the experimental set-up

Table 6 Summary of overall accuracy obtained from experimental set-up

Classification of the fault types	Number of case studies	Fault classification (%)		
		Trial-and-error method [19]	DWT and BPNN [35]	DWT and PNN
Single line-to-ground fault	30	70.00	90.00	96.67
Double line-to-ground fault	30	63.33	76.67	90.00
Line-to-line fault	30	83.33	90.00	93.33
Three-phase fault	10	60.00	70.00	80.00
Average		71.00	84.00	92.00

In addition, real data from a real-power system are not available for us to test the proposed scheme, but an experimental set-up was investigated. This experimental set-up was modelled after an actual transmission system in Thailand. Based on its accurate results for a simulation signal and real signal, it can be concluded that the proposed algorithm is adequate for other power systems with different line models and that it can be applied to actual systems even when the accuracy is slightly reduced by the effect of noise in the actual system. Thus, this verification shows the effectiveness of the proposed technique, which can perform accurately under various systems and fault conditions.

References

1. Costa FB, Souza BA, Brito NSD, Silva JACB, Santos WC (2015) Fault diagnosis of rotating electrical machines in transient regime using a single stator current's FFT. IEEE Trans Instrum Meas 64(11):3137–3146
2. Lima FPA, Lotufo ADP, Minussi CR (2015) Wavelet-artificial immune system algorithm applied to voltage disturbance diagnosis in electrical distribution systems. IET Gener Transm Distrib 9(11):1104–1111
3. Yao X, Herrera L, Ji S, Zou K, Wang J (2014) Characteristic study and time-domain discrete wavelet-transform based hybrid detection of series DC arc faults. IEEE Trans Power Electron 29(6):3103–3115
4. Alves HN, Fonseca Junior RNB (2014) An algorithm based on discrete wavelet transform for fault detection and evaluation of the performance of overcurrent protection in radial distribution systems. IEEE Latin Am Trans 12(4):602–608
5. Gritli Y, Lee SB, Filippetti F, Zarri L (2014) Advanced diagnosis of outer cage damage in double-squirrel-cage induction motors under time-varying conditions based on wavelet analysis. IEEE Trans Ind Appl 50(3):1791–1800
6. Devi NR, Sarma DVSSS, Rao PVR (2015) Detection of stator incipient faults and identification of faulty phase in three-phase induction motor–simulation and experimental verification. IET Electr Power Appl 9(8):540–548
7. Alshareef S, Talwar S, Morsi WG (2014) A new approach based on wavelet design and machine learning for islanding detection of distributed generation. IEEE Trans Smart Grid 5(4):1575–1583
8. Costa FB (2014) Boundary wavelet coefficients for real-time detection of transients induced by faults and power-quality disturbances. IEEE Trans Power Deliv 29(6):2674–2687
9. Costa FB (2014) Fault-induced transient detection based on real-time analysis of the wavelet coefficient energy. IEEE Trans Power Deliv 29(1):140–153
10. Seshadrinath J, Singh B, Panigrahi BK (2014) Incipient turn fault detection and condition monitoring of induction machine using analytical wavelet transform. IEEE Trans Ind Appl 50(3):2235–2242
11. Perveen R, Kishor N, Mohanty SR (2015) Fault detection for offshore wind farm connected to onshore grid via voltage source converter-high voltage direct current. IET Gener Transm Distrib 9(16):2544–2554
12. Li X, Dysko A, Burt GM (2014) Traveling wave-based protection scheme for inverter-dominated microgrid using mathematical morphology. IEEE Trans Smart Grid 5(5):2211–2218
13. Nouri H, Alamuti MM, Montakhab M (2016) Time-based fault location method for LV distribution systems. Electr Eng 98(1):87–96
14. Adly AR, El Sehiemy RA, Abdelaziz AY, Ayad NMA (2016) Critical aspects on wavelet transforms based fault identification procedures in HV transmission line. IET Gener Transm Distrib 10(2):508–517
15. Sharafi A, Sanaye-Pasand M, Jafarian P (2011) Ultra-high speed protection of parallel transmission lines using current travelling waves. IET Gener Transm Distrib 5(6):656–666
16. Yusuff AA, Jimoh AA, Munda JL (2011) Determinant-based feature extraction for fault detection and classification for power transmission lines. IET Gener Transm Distrib 5(12):1259–1267
17. Bo ZQ, Jiang F, Chen Z, Dong XZ, Weller G, Redfern MA (2000) Transient based protection for power transmission systems. In: IEEE power engineering society winter meeting, vol 3, pp 1832–1837
18. Youssef OAS (2001) Fault classification based on wavelet transforms. In: IEEE/PES transmission and distribution conference and exposition, vol 1, pp 531–538
19. Makming P, Bunjongjit S, Kunakorn A, Jiriwibhakorn S, Kando M (2002) Fault diagnosis in transmission lines using wavelet transform analysis. In: IEEE/PES transmission and distribution conference and exhibition 2002: Asia Pacific, vol 3, pp 2246–2250
20. Ngaopitakkul A, Kunakorn A (2006) Internal fault classification in transformer windings using combination of discrete wavelet transforms and back-propagation neural networks. Int J Control Autom Syst (IJCAS) 4(3):365–371

21. Perez FE, Orduna E, Guidi G (2011) Adaptive wavelets applied to fault classification on transmission lines. IET Gener Transm Distrib 5(7):694–702

22. Perez FE, Aguilar R, Orduna E, Guidi G (2012) High-speed non-unit transmission line protection using single-phase measurements and an adaptive wavelet: zone detection and fault classification. IET Gener Transm Distrib 6(7):593–604

23. Jiang J-A, Chuang C-L, Wang Y-C, Hung C-H, Wang J-Y, Lee C-H, Hsiao Y-T (2011) A hybrid frame work for fault detection, classification, and location part I: concept, structure, and methodology. IEEE Trans Power Deliv 26(3):1988–1998

24. Jiang J-A, Chuang C-L, Wang Y-C, Hung C-H, Wang J-Y, Lee C-H, Hsiao Y-T (2011) A hybrid frame work for fault detection, classification, and location part II: implementation and test results. IEEE Trans Power Deliv 26(3):1999–2008

25. Usama Y, Lu X, Imam H, Sen C, Kar NC (2014) Design and implementation of a wavelet analysis-based shunt fault detection and identification module for transmission lines application. IET Gener Transm Distrib 8(3):431–441

26. Dasgupta A, Nath S, Das A (2012) Transmission line fault classification and location using wavelet entropy and neural network. Electr Power Compon Syst 40(15):1676–1689

27. Livani H, Evrenosoglu CY (2014) A machine learning and wavelet-based fault location method for hybrid transmission lines. IEEE Trans Smart Grid 5(1):51–59

28. Seyedtabaii S (2012) Improvement in the performance of neural network-based power transmission line fault classifiers. IET Gener Transm Distrib 6(8):731–737

29. Roshanfekr R, Jalilian A (2016) Wavelet-based index to discriminate between minor inter-turn short-circuit and resistive asymmetrical faults in stator windings of doubly fed induction generators: a simulation study. IET Gener Transm Distrib 10(2):374–381

30. Li Y, Meng X, Song X (2016) Application of signal processing and analysis in detecting single line-to-ground (SLG) fault location in high-impedance grounded distribution network. IET Gener Transm Distrib 10(2):382–389

31. Guillen D, Paternina MRA, Zamora A, Ramirez JM, Idarrage G (2015) Detection and classification of faults in transmission lines using the maximum wavelet singular value and Euclidean norm. IET Gener Transm Distrib 9(5):2294–2302

32. Rajaraman P, Sundaravaradan NA, Meyur R, Reddy MJB, Mohanta DK (2016) Fault classification in transmission lines using wavelet multiresolution analysis. IEEE Potentials 35(1):38–44

33. El Safty S, El-Zonkoly A (2009) Applying wavelet entropy principle in fault classification. Electr Power Energy Syst 31:604–607

34. Silva KM, Souza BA, Brito NSD (2006) Fault detection and classification in transmission lines based on wavelet transform and ANN. IEEE Trans Power Deliv 21(4):2058–2063

35. Ngaopitakkul A, Bunjongjit S (2013) An application of a discrete wavelet transform and a back-propagation neural network algorithm for fault diagnosis on single-circuit transmission line. Int J Syst Sci 44(9):1745–1761

36. Ngaopitakkul A, Jettanasen C (2011) Combination of discrete wavelet transform and probabilistic neural network algorithm for detecting fault location on transmission system. Int J Innov Comput Inf Control 7(4):1861–1874

37. Bunjongjit S, Ngaopitakkul A (2012) Selection of proper artificial neural networks for fault classification on single circuit transmission line. Int J Innov Comput Inf Control 8(1):361–374

38. Aslan Y (2012) An alternative approach to fault location on power distribution feeders with embedded remote-end power generation using artificial neural networks. Electr Eng 92(3):151–134

39. Vyas BY, Das B, Maheshwari RP (2016) Improved fault classification in series compensated transmission line: comparative evaluation of Chebyshev neural network training algorithm. IEEE Trans Neural Netw Learn Syst 27(8):1631

40. Liu Z, Han Z, Zhang Y, Zhang Q (2014) Multiwavelet packet entropy and its application in transmission line fault recognition and classification. IEEE Trans Neural Netw Learn Syst 25(11):2043–2052

41. Chiradeja P, Ngaopitakkul A (2013) Prediction of fault location in overhead transmission line and underground distribution cable using probabilistic neural network. Int Rev Electr Eng 8(2):762–768

42. Chaiwat S (2010) Switching and transmission line diagram. Electricity Generating Authority of Thailand, Nonthaburi, Thailand

43. Daubechies I (1990) The wavelet transform, time-frequency localization and signal analysis. IEEE Trans Inf Theory 36(5):961–1005

44. Brito NSD, Souza BA, Pires FAC (1998) Daubechies wavelets in quality of electrical power. In: IEEE international conference on harmonics and quality of power, pp 511–515

45. Chiradeja P, Pothisarn C (2009) Identification of the fault location for three-terminal transmission lines using Discrete Wavelet Transform. In: Proceedings of IEEE international conference on transmission and distribution (T&D Asia 2009), vol 1, pp 1–4

46. Fausett LV (1994) Fundamentals of neural networks. Prentice-Hall, Englewood Cliffs

47. Haykin S (1999) Neural networks: a comprehensive foundation. Prentice-Hall, Englewood Cliffs